Model of holographic recording in amorphous chalcogenide films using subband-gap light at room temperature

A. Ozols
Institute of Solid State Physics, University of Latvia, LV-1063, Riga, Latvia

N. Nordman,* O. Nordman, and P. Riihola
Department of Physics, University of Joensuu, P. O. Box 111, FIN-80101, Joensuu, Finland

(Received 21 October 1996)

The subband-gap light holographic recording in amorphous as-evaporated As_2S_3 films at room temperature is experimentally studied. Properties are considerably different from those of usual holographic recording based on the band-gap light induced structural changes. The most important characteristic features of this nonpermanent recording include photoinduced refractive index increase, weak photobleaching, the absence of the photoinduced thickness changes, light polarization dependence, large exposures, holographic grating shifts during the exposure and a peculiar two maxima spatial frequency response. The first order diffraction efficiency up to 4.1% is achieved. These features as well as possible recording mechanisms are discussed. A subband-gap light holographic mechanism is proposed based on the photoinduced reorientation and generation of chalcogenide related D^- and D^+ centers counteracted by the photostimulated relaxational structural changes. The results obtained for amorphous As_2S_3 films can be applied also to other amorphous chalcogenide films. [S0163-1829(97)06021-9]

I. INTRODUCTION

Although amorphous chalcogenide films have been actively studied since the beginning of the 1970s,[1–5] they are still of large theoretical and practical interest because of the exciting disordered state physics involved and the numerous applications in the areas of real-time optical information storage,[2,4,5] holographic optical elements,[2] switching devices,[2,5] fibers,[6] waveguides,[6] coatings,[6] and photo-, x-ray, and electron beam lithography.[4] Real time holographic information storage is one of the most important applications of amorphous chalcogenide films. High spatial resolution of about 10 000 lines/mm,[7] the simplicity of a direct recording process, reversibility, and the availability of large samples are some of the attractive features of these materials.

Usually band-gap or superband-gap light is used for the hologram recording in amorphous chalcogenide films.[2,4] In this case the holographic recording is based on photoinduced structural changes (PSC). It enables efficient and practically permanent holograms.[2,4,6,7] However, we have found that holographic recording by subband-gap light is also possible. A different recording mechanism is involved. The properties of this recording process are very different from the processes based on PSC.

In this article we describe and explain the results of the experimental studies of the subband gap light holographic recording in amorphous As_2S_3 films (a-As_2S_3 films). In order to have a good background different previously known physical recording mechanisms are reviewed in Sec. II. In Sec. III we describe our experimental setup and display the measured data. In Sec. IV we discuss the measured data and compare them to the known recording mechanisms. In this section we suggest also a mechanism for the subband gap holographic recording. This mechanism is based on the photoinduced reorientation and generation of chalcogenide related D^- and D^+ centers (valence-alteration pairs) counteracted by the photostimulated relaxational structure changes. Conclusions are made in Sec. V.

II. MECHANISMS OF HOLOGRAPHIC RECORDING IN AMORPHOUS CHALOGENIDE FILMS

A. Photostructural changes

PSC is a unique phenomenon found only in noncrystalline chalcogenide materials.[2–5] Band-gap or superband-gap light is necessary for PSC.[2–5] However, one can expect weak PSC also when subband-gap light is used because of the spatial fluctuations in the band edges.[1] It is widely acknowledged that PSC means a metastable shift of the atoms as a result of the photoinduced bond switching.[2,4,5,8] Such a shift is possible because of the lattice nonrigidity of the films. This is due to the average coordination number Z of these films. For a-As_2S_3, $Z=2.4$,[9] the condition $Z<2.67$ being necessary for the topological nonrigidity.[10] The concentration of the soft atomic configurations is estimated to be $\sim 10^{21}$ cm^{-3}.[11] PSC express themselves by changes of the absorption coefficient (photodarkening at the room temperature), refractive index, thickness, density, microhardness, and dissolution rate.[2,6,8] The structure changes at both short range and intermediate range levels.[2–4,8] Infrared[8] and EXAFS (Ref. 12) spectroscopic studies of nonannealed a-As_2S_3 films have shown that band gap light induced PSC are mainly due to the As-As bond breaking[13] followed by the phonon-assisted creation of As-S bonds. The process is described by the reaction[8]

$$2\,As_3 + S_3^0 \rightleftarrows^{\hbar\omega} As_2^+ + As_2^- + S_2^0 \rightleftarrows^{kT} As_3^0 + S_3^+ + As_2^- . \quad (1)$$

Here the upper indices designate the electric charge of the atoms and the lower ones their coordination numbers. More

precisely, the photons with the energy $\hbar\omega \approx E_g$ [$E_g = 2.39$ eV (Ref. 14)] in the Franck–Condon process[11] break ''wrong'' As-As bonds. After that phonon-assisted As-S donor-acceptor bond formation takes place using the lone-pair (LP) π electrons of S_2^0 atoms.[2,4,8] The analogous reaction for amorphous As-Se films has been proposed in Ref. 15. The inverse direction of reaction (1) proceeds with lower speed.

The reaction of Eq. (1) leads to the densification of the structure of the films. According to the neutron and x-ray diffraction data as-evaporated a-As_2S_3 films are packed by almost spherical cagelike As_4S_4 molecules containing As-As bonds.[16] The molecules are kept together only by weak van der Waals forces.[16] The reaction of Eq. (1) induce crosslinking between the As_4As_4 molecules. As a result the whole network becomes more rigid as shown by density[2,4] and microhardness increase and the thickness decrease.[17]

If photons with $\hbar\omega > E_g$ or elevated temperatures are used[4] the mechanism of PSC can be quite different (Sec. II C).

B. Relaxational structural changes

Holographic recording in amorphous chalcogenide films based on PSC is strongly affected by relaxational structural changes (RSC). RSC lead to the relaxational self-enhancement of holograms,[18] existence of recording intensity threshold,[19] nonlinearity of exposure curves,[20,21] changes in spatial frequency response in the course of the aging of the films, and also to other effects.[21] As RSC can be stimulated by light[22,23] the holographic recording based on RSC is also possible.

RSC are inherent in all noncrystalline materials due to their thermodynamic instability.[24] When a-As_2S_3 films are thermally deposited in vacuum on the glass substrates some excess free energy is stored into films because of the strain-induced topological structural disorder,[25] compositional disorder,[26] and nonhomogeneity.[27] This stored excess energy decreases with time owing to RSC. The driving force behind the RSC are the internal mechanical stresses arising during the thermal deposition and diminishing in the course of relaxation.[16–21,27] RSC are facilitated by the nonrigidity of the lattice.

Although heating of the films up to $\sim$100 °C accelerate RSC,[27] they are strong even at room temperature.[18] Only the intermediate range order structure changes during the RSC at room temperature.[28] This means that there is no bond breaking but only the changes in the bond angles and the shift of atoms. The main role in a-As_2S_3 films is played by the sulphur atoms.[3,18]

Amorphous chalcogenide films relax towards more ordered structural states as shown by their densification and increase in the slope of Urbach's absorption edge [$\hbar\omega < 2.4$ eV in a-As_2S_3 (Ref. 3]. The latter mainly but not completely[1,29] corresponds to the transitions between the localized Urbach's tail states near the valence band and the conduction band edges.[3,29] Above the top of the valence band these localized states are mainly due to the distortion of the bond angles.[30] The band tail is the consequence of the bond length and bond angle distortions frozen in at glass transition temperature.[25] Therefore, a steeper slope corresponds to smaller distortion.[30] The Urbach's edge is also the spectral region where the PSC induced photodarkening expresses itself in the form of a parallel shift in the edge towards lower photon energies.[3] RSC result in a decrease of absorption and thickness[6] as well as increase of refractive index,[6,27] density,[6] microhardness,[26] and dissolution rate.[27]

It is experimentally found that subband-gap light strongly decreases the viscosity of a-As_2S_3 glass[21,22] and this decrease proceeds exponentially as the light intensity is increased.[22] Evidently, this occurs because of the photoexcitation of weak van der Waals bonds connecting the molecular fragments.[4]

If a holographic grating is recorded by a periodical light intensity distribution it spatially modulates the viscosity and hence the internal mechanical stress. Using the theory of elasticity the stress modulation amplitude $\Delta\sigma$ is found to be directly proportional to the films thickness d and inversely proportional to the grating period Λ (Refs. 18 and 31)

$$\Delta\sigma \propto \frac{d}{\Lambda}. \tag{2}$$

Periodical mechanical stress modulation with the amplitude qualitatively obeying Eq. (2) is created during the PSC-based recording in amorphous chalcogenide films.[18,21] We have successfully used the periodically distributed stress relaxation (PDSR) model to explain the numerous peculiarities of these experiments partially mentioned in the beginning of this section.

The spatially modulated internal stress causes periodical refractive index changes directly through the elastooptic effect and indirectly through the stress induced displacements of atoms without breaking the chemical bonds. In the latter inelastic case the displacement of atoms enables a directed relaxational motion of unfilled sites (pores, voids, vacancies) from the grating maxima to minima or vice versa depending on the sign of $\Delta\sigma$. This results in density and refractive index modulation which either increases ($\Delta\sigma > 0$) or decreases ($\Delta\sigma < 0$) the refractive index modulation due to the PSC.[18–21]

The PDSR model can also be applied when subband-gap light is used for the recording. In that case one has to take into account that due to the photoinduced viscosity decrease the stress maxima correspond to the light intensity minima. In other words, the holographic grating recorded by RSC is in counterphase with respect to the recording intensity pattern and the refractive index change is negative.[20–23] Equation (2) can be still regarded as a ''fingerprint'' of RSC.

C. Recharging of localized states

The photoinduced recharging of the localized states which have energy levels in the band gap can be used for the holographic recording. The sign and spectral dependence of the photoinduced changes in absorption coefficient and refractive index depend on the exciting photon energy.

If band-gap or superband-gap light is used a broad transient absorption band (living seconds) appears in a-As_2S_3 films centered around 2.39 eV at room temperature.[32] The corresponding refractive index changes are due to the excitation of electrons trapped in normally unoccupied states near the valence band edge.[32] These processes can be used for transient hologram recording.

The recharging of the localized states of D^0, D^+, D^- centers[1] in As-S glass have been used for the holographic recording at elevated temperatures by subband-gap (He-Ne laser, wavelength $\lambda=632.8$ nm) light.[34] The first order diffraction efficiency up to 90% have been achieved. A theory is developed to explain the obtained results.[34,35] According to this theory four different holographic grating types can be formed depending on temperature (T). First, at $T>50$ °C a hole (As-S is a p-type semiconductor[1]) polaron grating is recorded where D^0 centers are formed in the intensity maxima as a result of photothermal recharging process. This grating is not shifted with respect to the recording interference pattern (phase shift $\Phi=0$). Second, a shifted ($\Phi\neq0$) hole bipolaron grating is recorded at $T=50-100$ °C due to the diffusion of the hole polarons, their drift and recharging of different localized levels. It consists of alternating D^+ and D^- centers in the grating maxima and minima. Third, a shifted ($\Phi=\pi$) grating is recorded at $T\geqslant110$ °C under the certain additional conditions. It is formed by the pairs of D^+ and D^- centers in the interference minima.[34] Fourth, a shifted ($\Phi=\pi$) grating is recorded due to the photoinduced diffusion of D^0 centers at $T>120$ °C to the interference pattern minima.

The real holographic recording is found to be the superposition of all the described processes. The characteristic features of this recording are large refractive index changes ($\Delta n=0.1-0.2$) and small absorption coefficient changes ($\Delta\kappa=2\times10^{-3}$ cm^{-1}) at the recording wavelength. Also the intensity dependence and the decrease of the efficiency with the increasing grating period belong to these features. All the described grating types except the first one are stable at the room temperature since they are actually recorded due to another type of PSC initiated by the recharging of localized levels.[34,25] The first type holographic grating is unstable because there is no PSC and the reaction

$$2D^0\rightarrow D^+ + D^- \tag{3}$$

is exothermic.[1,34] It is also found that the induced D^0, D^+, and D^- centers are chalcogen related centers D^0 corresponding S_1^0 or S_3^0, D^+ corresponding S_3^+ and D^- corresponding S_1^-.[34]

It seems that photoinduced recharging of chalcogen related defects followed by the PSC as described above can be the mechanism for the giant photoexpansion of As_2S_3 glass[36] and for the photoinduced Bragg gratings in As_2S_3 optical fibers[37] because intense 632.8 nm laser light (10^4 and 14 W/cm^2) with long exposures ($\sim10^3$ s and 2–5 h) was used in both cases.

D. Photoinduced anisotropy

Birefringence ($\sim3\times10^{-3}$) in a-As_2S_3 films induced by a linearly polarized Ar^+ laser beam with the wavelength $\lambda=514.5$ nm was measured already in 1977.[38] Photoinduced anisotropy can be induced efficiently by subband-gap light as shown by experiments with As_2S_3 glass.[3,39–41] It turned out that linearly polarized light causes not only a linear dichroism and birefringence but also a circular dichroism and birefringence so that generally we have an elliptical photoinduced dichroism and birefringence.[39,40] This concerns also the anisotropy induced by circularly polarized light.[40] The linear photoinduced dichroism changes not only its magnitude but also its sign during the exposure thus revealing the complexity of the process.[39,41]

Most efficiently the linear dichroism can be induced by red ($\lambda\leqslant627$ nm) light corresponding to the excitation of states in Urbach's tail.[41] The spectral dependence of the photoinduced dichroism exhibits a maximum at wavelengths longer than the exciting wavelength. During the exposure the maximum is gradually shifted towards the inducing wavelength.[41] The Urbach's tail states are shown to be responsible for the photoinduced anisotropy.[3,41]

The properties of photoinduced anisotropy remarkably differ from those of PSC.[3,40] Unlike the PSC in a-As_2S_3 films sulphur atoms are found to play the major role in photoinduced anisotropy as shown by XAFS (Ref. 3) and EXAFS (Refs. 12 and 40) measurements. It is known that subband-gap light predominantly induces chalcogen related defects.[3] The top of the valence band of chalcogenide materials is comprised of LP π-electron states associated with nonbonding chalcogen orbitals.[3] Evidently, the photoexcitation of these LP electrons starts the photoanisotropy effect.[3]

It is believed that photoinduced anisotropy is due to the photoinduced reorientation[3,42,43] of the native anisotropic defects or the generation[3,39,41] of the new ones. The photoinduced reorientation proceeds faster than the generation.[42] Recently a model was developed in order to explain the great influence of the photoinduced anisotropy.[43] The model is based on the reorientation of the valence alteration pairs (VAP of D^+ and D^- centers[1]). In spite of the modest concentration of VAP [$\sim10^{17}$ cm^{-3} (Refs. 1 and 34)] a strong interaction of VAP with their environment[1,3,4] was assumed.[43] However, the microscopic mechanism of photoinduced anisotropy is not yet clear.

III. EXPERIMENTS AND RESULTS

Thin a-As_2S_3 films were thermally evaporated in vacuum (5×10^{-4} Pa) at room temperature onto optical K-8 glass substrates at the deposition rate of 80 Å/s. The thickness ($d=11$ μm) of 3×3 cm^2 films was measured interferometrically during the deposition. The stoichiometric As_2S_3 composition of the nonannealed film was checked by neutron activation analysis. Before the recording the films were kept in the dark at room temperature for about two years.

Mainly holographic experiments have been carried out. Transmission holographic gratings with periods $\Lambda=0.4$, 0.5, 0.7, 1.0, 5.0, 10.0, and 20.0 μm were recorded by two symmetrically incident s-polarized He-Ne laser beams ($\lambda=632.8$ nm) of equal intensity. The $1/e^2$ Gaussian laser beam diameter was 1.10 mm. The readout wavelength was 632.8 nm. So the recording photon energy $\hbar\omega=1.96$ eV was less than the optical band gap $E_g=2.39$ eV.[14] The average intensity of both recording beams were varied between 0.03–0.04 W/cm^2. However, in most experiments the intensity was 0.23 W/cm^2. Each set of Λ measurements was recorded in the same 3×3 cm^2 film in order to minimize the errors caused by possible differences in physical properties between different 3×3 cm^2 films.

The first order diffraction efficiency η_1 of the holographic gratings was measured in real time by blocking one of the recording beams for one second every 240 seconds. In all

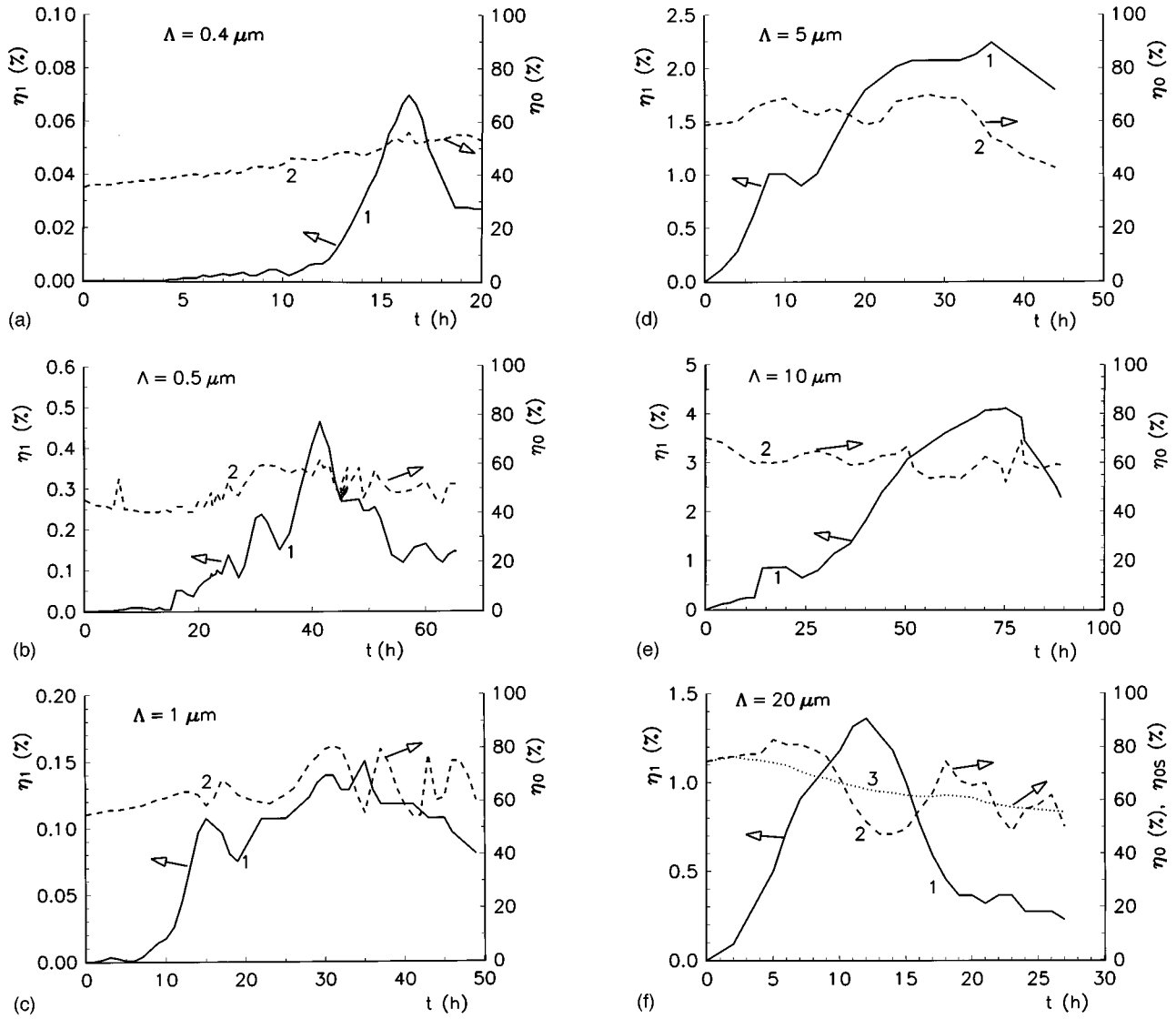

FIG. 1. The first-order (η_1) and the zeroth-order (η_0, η_{0s}) diffraction efficiencies as functions of the exposure time at $I=0.23$ W/cm^2 and $\lambda=632.8$ nm. Grating period Λ was varied and they are displayed in the figure.

cases the zeroth order diffraction efficiency η_0 was measured continuously.

Special care was taken to stabilize the holographic setup because of the long exposure times up to 90 h. We have proved the stability of our holographic setup using an energy exchange effect between the two coherent light beams diffracted in the zeroth order by a phase grating. The effect takes place when the grating is shifted with respect to the interference pattern of the beams by a distance Δ.[44] The zeroth order diffraction efficiencies for two equal intensity simultaneously incident beams are related by the equation[44]

$$\eta_0 = \eta_{0s}[1+\hat{\eta}_1 \pm 2(\hat{\eta}_1)^{1/2}\sin\Phi]. \quad (4)$$

Here $\hat{\eta}_1 = \eta_1/\eta_{0s}$ and η_{0s} is the value of the zeroth order diffraction efficiency measured simultaneously with η_1. The angular spatial frequency of the grating $\Phi = K\Delta$ and $K = 2\pi/\Lambda$. Measuring η_0 versus time dependences of both beams using dichromated gelatin phase grating ($\Lambda=1.9$ μm, $\eta_1=0.40$, $\hat{\eta}_1=1.07$) we have found that typically Δ does not exceed 0.4 μm within 12 h.[19]

Apart from holographic experiments we have measured transmittance (T) and reflectance (R) as a function of time for a single normally incident beam. Optical absorption spectra were obtained and possible photoinduced thickness variations were tested with the profilometer (Tencor Alpha-Step 500). The quantitative experimental results are presented in Figs. 1–4 and Table I.

The relative error in our measurements did not exceed 5% for η_1, η_0, T, R measurements, 2% for the Λ measurements, and 1% for optical density (D) measurements. The absolute error of differential optical density (ΔD) measurements did not exceed 0.03.

Due to the low absorption of a-As_2S_3 samples at $\lambda=632.8$ nm long exposures times up to 90 h were necessary to read the η_1 maxima as seen in Figs. 1(a)–1(f). Corresponding recording energies $W = It\eta^{-1}$ (t is the exposure time and η is the diffraction efficiency) varied in 1×10^4–1×10^5 J/cm^2 %) range which is several orders of magnitude more than for the PSC-based recording by Ar^+ laser at $\lambda=514.5$ nm in similar samples. Nevertheless, rea-

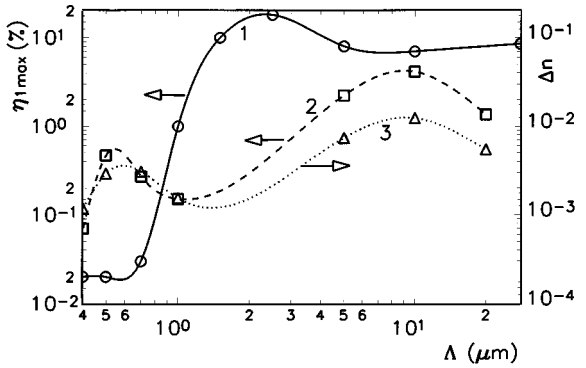

FIG. 2. Curve 1: The measured maximum of the first order-diffraction efficiency ($\eta_{1\max}$) as a function of grating period Λ for the PSC-based recording ($\lambda=514.5$ nm). All the gratings were read by the 632.8 nm line. Curve 2: The measured maximum of the first order diffraction efficiency ($\eta_{\max}$) for the subband-gap light recording by the 632.8 nm He-Ne laser line. Curve 3: The refractive index change $\Delta n=2n_1$ for the He-Ne recording. The values were calculated from $\eta_1, \eta_0, \eta_{0s}$ exposure dependencies (Fig. 1) using Eqs. (9) and (10).

sonable diffraction efficiencies η_1 up to 4.1% have been achieved. The oscillations of η_1, $\eta_0, \eta_{\rm os}$ specific for the 632.8 nm recording are observed (Fig. 1).

The grating period dependence of $\eta_{1\max}$ is quite different from that of PSC-based recording (Fig. 2). There are two $\eta_{1\max}$ maxima for the 632.8 nm recording at $\Lambda=0.5$ and 10 μm whereas there is only one maximum at $\Lambda=2$ μm for Ar^+ laser recording.

Transmittance and reflectance exposure versus time dependencies exhibit oscillatory behavior (Fig. 3). This is due to the Fabry-Pérot resonator effect in thin films. When the refractive index is changing the intensities of transmitted and reflected beams are changing due to the interference of multiple internally reflected beams with varying phases.[45] The effect is also realized by the optical density oscillations versus the wavelength in Fig. 4. Oscillations cannot be detected in the wavelength range of the high absorption, because the beams which have propagated through the film are strongly suppressed.

The phase character of the holographic gratings in a-As_2S_3 films recorded and read out by the 632.8 nm line is

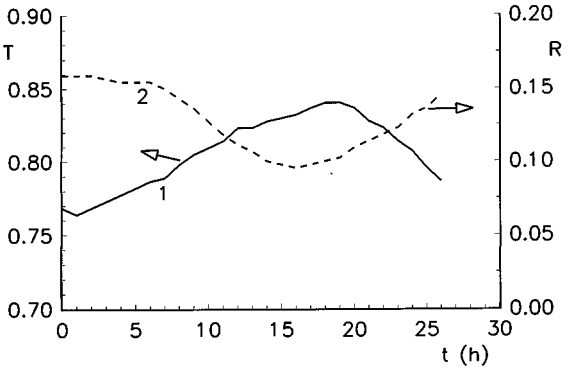

FIG. 3. Transmittance T and reflectance R as a function of time for normally incident single beam exposure at $I=0.115$ W/cm^2 and $\lambda=632.8$ nm.

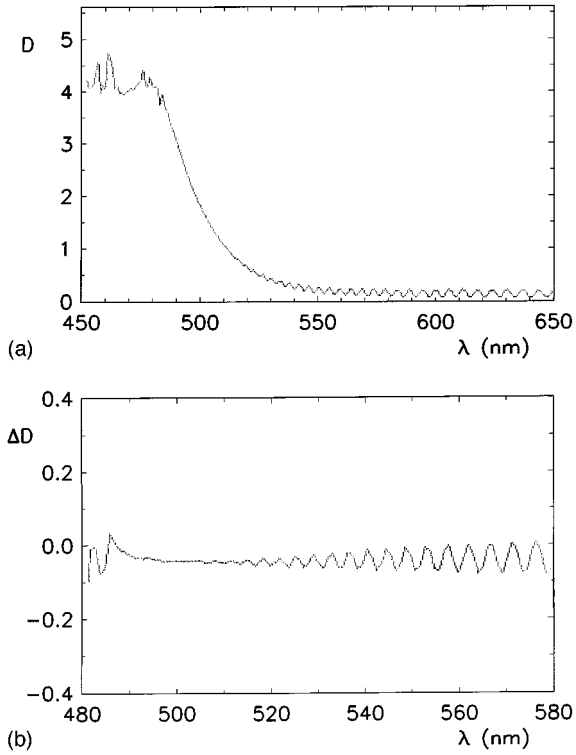

FIG. 4. Absorption spectra of the a-As_2S_3 film. (a) Spectrum before the exposure. D is the optical density. (b) Change in the optical density (ΔD) caused by the sinusoidal light intensity distribution with $\lambda=632.8$ nm, $\Lambda=0.7$ μm, $I=0.23$ W/cm^2, and time $=19.1$ h.

confirmed by following experiments. We have observed grating shift induced energy exchange effect between the two unblocked recording beams described by Eq. (4) during the exposure time of 50 h. No energy exchange is possible for amplitude gratings because the diffracted first order beam is then phase-shifted by π with respect to zero-order beam whereas a $\pi/2$ phase shift takes place for phase gratings.[44,46] We have observed this $\pi/2$ shift of the interference pattern (using a microscope objective) when one beam was blocked (in the blocked position the interference pattern is created by zero-order and first-order diffracted beams and a $\pi/2$ phase shift again corresponds to phase gratings[47]). From the direction of the displacement of the interference pattern we have determined the sign of the refractive change to be positive.

The exposed areas were scanned through with the profilo-

TABLE I. Characteristics of the holographic gratings recorded in a-As_2S_3 films by the 632.8 nm light with $I=0.23$ W/cm^2.

Λ (μm)	$t_{\max}$ (h)	$\eta_{1\rm av}$ (%)	$\eta_{1\max}$ (%)	$\eta_{1\max\,\rm opt}$ (%)	$\Delta n(10^{-3})$
0.40	16.3	0.040	0.070	0.071	1.18
0.50	42.3	0.180	0.47	0.47	2.9
0.70	38.1	0.130	0.27	0.48	3.1
1.0	34.3	0.100	0.15	0.15	1.54
5.0	34.0	1.8	2.2	3.6	7.4
10.0	78.4	2.7	4.1	12.7	12.4
20.0	12.2	0.88	1.4	2.2	5.5

meter. As we have found no photoinduced thickness changes we concluded that 632.8 nm light causes the refractive index increase.

Fabry-Pérot resonator effects and grating shifts with respect to the recording interference pattern are characteristic features of the holographic recording in a-As_2S_3 films by the 632.8 nm He-Ne laser light. The grating shift has no effect on η_1 and η_{0s},[48] but it has an influence on η_0 according to Eq. (4). The Fabry-Pérot resonator effect influences all the values of $\eta_1, \eta_0, \eta_{0s}$ depending on the current refractive index medium value.[45] Therefore it was necessary to take this effect into account in order to find the refractive index changes corresponding to the measured $\eta_{1\max}$ values and the highest possible $\eta_{1\max}$ values. These were calculated and are presented as $\eta_{1\max\,\mathrm{opt}}$ in Table I. The theory of thin absorbing phase gratings with multiple internal reflections was used in calculations.[45] According to the Q factor[46] it can be applied only starting from $\Lambda=5$ μm. However, for small enough $\eta_1<8\%$ the theoretical results for the diffraction efficiencies η_1 and η_{0s} of thick[46] and thin[48] gratings are the same within 5% accuracy. Therefore the use of the thin grating theory is justified also for $\Lambda=0.4$–1 μm. Further we neglect the oblique incidence of the beams inside the film at the angle θ_i assuming $\cos\theta_i=1$. Because of the large refractive index of a-As_2S_3 films ($n=2.45$ at 632.8 nm) this approximation causes less than 0.5% errors on η_1, and η_{0s} values.

A sinusoidal recording light intensity distribution induces the first Fourier harmonic refractive index modulation:[49]

$$n=n_0+n_1\cos(Kx). \tag{5}$$

Here n_0 is the refractive index of the medium, n_1 is the refractive index modulation amplitude averaged over the grating area and thickness. x is a coordinate along the film surface. The corresponding modulation of the phase thickness

$$\delta=\frac{4\pi}{\lambda}nd \tag{6}$$

is

$$\delta=\delta_0+\delta_1\cos(Kx). \tag{7}$$

Rearranging the results of Ref. 45 to our case we get the following formula for the pth order ($p=0,1$) diffraction efficiency taking into account multiple internal reflections:

$$\eta_p=(1-R_1)(1-R_2)(1-R_3)\exp(-\kappa d)\left[\sum_{s=0}^{\infty}(R_1R_2)^s\exp(-2s\kappa d)J_p^2\left(\frac{2s+1}{2}\,\delta_1\right)\right.$$
$$\left.+2\sum_{l=0,l<s}^{\infty}(R_1R_2)^{0.5(s+l)}\exp[-(s+l)\kappa d]J_p\left(\frac{2s+1}{2}\,\delta_1\right)J_p\left(\frac{2l+1}{2}\delta_1\right)\cos[(s-l)\delta_0]\right]. \tag{8}$$

Here R_1, R_2, R_3 are the Fresnel reflection coefficients of the air-film, film-substrate and substrate-air interfaces, κ is absorption coefficient, and $J_p(\alpha)$ is the Bessel function of the first kind and the $p$the order. In Eq. (8) the reflections from the substrate-air interface are neglected due to their weakness.

To simplify Eq. (8) we keep only the first terms in each infinite sum because R_1R_2 is a small quantity ($\sim$0.01). Further, because of the small phase thickness modulation amplitude δ_1 we can expand $J_p(\alpha)$ in series keeping only the first terms. These approximations for $J_p(\alpha)$ are valid if $\delta_1<1.33$ and cause the error not exceeding 37% in the worst case for all grating periods except $\Lambda=10$ μm. The mathematical error in η_p corresponding to the 37% $J_p(\alpha)$ error does not exceed 7%.

In the case of $\Lambda=10$ μm one should have taken into account also the second terms in $J_p(\alpha)$ series. However, calculations according to Eq. (8) including the second terms in $J_p(\alpha)$ expansions show that a periodical n modulation [Eq. (5)] decreases the influence of the Fabry-Pérot resonator effect and the $\eta_{0s}(\delta_0), \eta_0(\delta_0), \eta_1(\delta_0)$ dependencies should be strongly weakened. Nevertheless we did not observe this kind of weakening in the strongest n-modulation cases [Figs. 1(d)–1(f)]. This is due to the Gaussian shaped light intensity distribution. Using the theory developed in Ref. 45 for the holographic gratings recorded and probed by Gaussian beams one can show that in our case the influence of the grating on the Fabry-Pérot effect is significantly reduced. However, we do not use this theory because it is much more complicated and does not add new features. Gaussian light intensity distribution reduces all the higher terms relative to the first one [Eqs. (10) and (16) in Ref. 45]. Physically it means the reduction of the grating influence on the Fabry-Pérot effect. Therefore the neglect of the second terms in the $J_p(\alpha)$ expansions in our case is reasonable. Taking into account the above approximations we get from Eq. (8)

$$\eta_1=(1-R_1)(1-R_2)(1-R_3)\exp(-\kappa d)\times\frac{\delta_1^2}{16}[1+6(R_1R_2)^{1/2}\exp(-\kappa d)\cos\,\delta_0], \tag{9}$$

$$\eta_{0s}=(1-R_1(1-R_2)(1-R_3)\exp(-\kappa d)\times[1+2(R_1R_2)^{1/2}\exp(-\kappa d)\cos\,\delta_0]. \tag{10}$$

In our experiment $R_1=0.18$, $R_2=0.058$, and $R_3=0.04$. The factor $\exp(-\kappa d)$ varied from 0.60 to 0.95 depending on the sample. Within the given accuracy $T=\eta_{0s}$.

During the exposure δ_0 is growing and η_1, η_{0s} oscillate due to the Fabry-Pérot resonator effect according to Eqs. (9) and (10). Calculations show that the oscillation amplitude could reach 50% of the medium level for η_1 and 18% for

η_{0s} showing the significance of the effect (Figs. 1 and 3). Using $\eta_1, \eta_0, \eta_{0s}$ exposure times dependencies (Fig. 1) and Eqs. (9) and (10) we found the $\eta_{1\max}$ values optimized with respect to δ_0 and the n_1 values corresponding to $\eta_{1\max}$. In the cases when the η_{0s} time dependencies were not explicitly available we have used the medium level values of η_0. One can see from Fig. 1(f) that such approach is reasonable. The average $\eta_{1\max}, \eta_{1\max\,\mathrm{opt}}, \eta_{1\mathrm{av}}$ (the average value of three measurements) values and the exposure times $t_{\max}$ corresponding to $\eta_{1\max}$ are presented for different grating periods Λ (Table I). Also the refractive index changes $\Delta n = 2n_1$ corresponding to $\eta_{1\max}$ are shown in the table. The estimated accuracy of $\eta_{1\max\,\mathrm{opt}}$ and Δn values is about 30% and 5%, respectively. It is seen that Δn varies in the 10^{-3}–10^{-2} range and noticeably higher $\eta_{1\max}$ values are possible for appropriate δ_0.

In our experiments we have not found any intensity dependence for the 632.8 nm holographic recording at $I = 0.03$–0.04 W/cm^2. Neither we found any self-enhancement of the diffraction efficiency. Instead we noticed that samples were photobleached by photons of $\lambda = 633$ nm and that the gratings were not permanent. The diffraction efficiency was decaying by a factor of 10 in two days.

We have observed a strong influence of the recording beam polarizations. The change of the polarization of one beam quickly changed the current η_1 value indicating similar mechanisms as mentioned in Ref. 43. However, a more detailed analysis remains to be done.

IV. DISCUSSION

Before discussing the mechanism of the subband-gap light holographic recording in a-As_2S_3 films let us consider more closely some relevant experimental details. We have found from our measurements that the absorption coefficient κ of our films at $\lambda = 632.8$ nm varied in the wide range from 50 to 460 cm^{-1} depending on the sample. Most frequently we had $\kappa = 200$–300 cm^{-1} which is much more than previously is mentioned.[1,39,40] In our opinion there are two possible reasons for that. There may be some preliminary photodarkening during the film preparation process because it was not carried out in complete darkness. Residual laboratory lights during the experiments may also lead to some permanent and transient photodarkening. We have observed transient absorption increase by about 270 cm^{-1} when all the room lights were switched on. This is due to the band-gap light recharging of the localizes states (Sec. II C). Evidently, the increased absorption enabled the holographic recording in our a-As_2S_3 films by 632.8 nm light.

Let us discuss the time dependencies of the diffraction efficiencies η_1, η_0, and η_{0s}. The first order diffraction efficiency η_1 is growing due to the n_1 increase and then it decreases due to the Δn saturation which leads to the decrease of n_1.[49] Oscillatory η_1, η_0, and η_{0s} time dependencies are the characteristic features of the 632.8 nm recording in a-As_2S_3 films (Fig. 1). Comparing Figs. 1 and 3 as well as η_0 and η_{0s} time dependencies in Fig. 1(f) one can see that slow η_0 and η_{0s} are due to the Fabry-Pérot resonator effect described by the $\cos\delta_0$ term in Eqs. (9) and (10). The fast observed η_0 oscillations are evidently due to the grating shifts and the competition of recording processes in the film [Fig. 1(f)]. It leads to n_0 changes. Besides, holographic grating shift directly changes η_0 via the interference of recording beams according to Eq. (4). Grating shifts are responsible for the fast η_1 oscillations since the period of the fast oscillations is growing when Λ is increased (Fig. 1).

Generally, there can be three reasons for grating shifts: (i) holographic setup instabilities, (ii) repeated blocking of one recording beam,[50] and (iii) the recording mechanism. Although we have maximally stabilized the holographic setup the instabilities are clearly present during the long exposure times up to 90 h. However, their existence does not explain all the observed peculiarities. The change of the sample holders of different constructions did not have noticeable effect. The $\eta_{1\max}$ versus Λ increase is not monotonical as can be expected (Fig. 2). Also there are large η_0 oscillations accompanied by a slowly varying η_{0s} time dependence in 20 h even for $\Lambda = 20$ μm [Fig. 1(f)]. Using Eq. (4) we found that the grating shift Δ in this case exceeded 5 μm. This is much more than $\Delta \approx 1$ μm which can be due to the setup instability[19] (Sec. III). Therefore, the holographic setup instability is not the only reason for grating shifts.

Repeated blocking of one recording beam also caused grating shifts[50] in our experiments. Due to the large duty cycle (beam interruption for one second every 240 seconds) we do not expect this effect to be significant. Besides similar η_0 oscillations were observed also in the cases when both beams were opened all the time.

Taking into account the above considerations we conclude that there should be some grating shift during the exposure because of the recording mechanism. However, the origin of this shift is not clear.

The holographic subband-gap light recording mechanisms in amorphous chalcogenides is known to be lead to shifted gratings[34,35] (Sec. II). The mechanisms are based on the photoinduced recharging of D^0, D^+, and D^- centers at temperatures exceeding 50 °C. Therefore, they cannot be efficient at room temperature. Besides, in all of these mechanisms diffusion processes are involved except in the formation of D^0-polaron gratings. This means that their efficiency should decrease when the grating period is increased. According to Fig. 2 our gratings behave differently. Either we have not found a prominent intensity dependence characteristic for the D center recharging. Most probably only unstable D^0 polaron grating formation can contribute to the 632.8 nm light holographic recording in a-As_2S_3 films. Yet this mechanism can only have minor influence.

The recharging of unfilled traps by the band-gap light excitation[32,33] is improbable because $\Delta\kappa$ should be positive[32] and Δn negative.[33] However, we have observed opposite $\Delta\kappa$ and Δn signs (Sec. III).

The properties of the 632.8 nm holographic recording are also different from those of the Ar^+ laser ($\lambda = 514.5$ nm) recording when PSC occur. The characteristic features of PSC based recording include photodarkening, photoinduced thickness changes, thermal stability at room temperature, coherent self-enhancement effect,[47] and the absence of the grating shift.[51] The opposite features are characteristic for the 632.8 nm recording (Sec. III). Therefore, the contribution of PSC can be ruled out.

From the holographic recording mechanisms in amorphous chalcogenide films only the photostimulated RSC and

the photoinduced anisotropy effect can give a significant contribution to the 632.8 nm recording in a-As_2S_3 films. Both of them are effectively stimulated by 632.8 nm light whose photon energy corresponds to the Urbach's tail states. The interaction includes the changes in the position or states of the sulphur atoms. Photostimulated RSC (Ref. 52) and photoinduced anisotropy are polarization sensitive. They exhibit relatively larger refractive index changes than absorption changes at $\lambda=632.8$ nm.[27,41] This feature is specific to the photoinduced processes involving sulphur related D-center transformations[34,35] (Sec. II). So we conclude that both processes of photostimulated RSC and photoinduced anisotropy contribute to the subband-gap light holographic recording in a-As_2S_3 films at $\lambda=632.8$ nm.

We propose a holographic recording mechanism where the grating constructed by the photoinduced reorientation and generation of D centers is partially destroyed by the photostimulated RSC. The proposed mechanism works as follows. When a spatially periodic light intensity distribution is applied to the film the photoinduced reorientation and generation of D centers takes place leading to the refractive index increase which is proportional to the exposure. The photostimulated RSC proceed via the excitation of the intermolecular van der Waals bonds[3,39] relaxing the internal mechanical stress and shifting the atoms mainly in light intensity maxima. This leads to the viscosity decrease and to negative refractive index changes[20,21] according to the PDSR model (Sec. II). This results in the refractive index modulation which is in counterphase to that created by the photoinduced reorientation and generation of D centers. In spite of the negative refractive index changes photostimulated RSC cannot be the dominating recording mechanism because there are no thickness changes and the recording is unstable. These two features are otherwise typical for the RSC. So the role of photostimulated RSC is only destructive. The two competing processes can lead to the nonmonotonical changes in the refractive index modulation amplitude which are seen as fast η_1 oscillations in Fig. 1

Let us examine in more details the photoinduced reorientation and generation of D centers responsible for the grating buildup. We know that subband gap light is able to generate the chalcogen related D centers.[3] We assume that D^- and D^+ centers are involved. These centers correspond to the sulphur defects S_1^- and S_3^+. As mentioned in Sec. II the photoinduced reorientation of D^- and D^+ centers was suggested[42,43] to explain the effect of photoinduced anisotropy. D^0 centers are unstable due to the reaction of Eq. (3). The main role is played by the reorientation of D^- centers, i.e., of the S_1^--type dangling bonds. As for D^+ centers their reorientation needs the photoinduced bond switching and this seems to be less efficient process at room temperature. The conclusions presented above are supported by the fact that the photoinduced reorientation process is faster[42] and more polarization dependent than photoinduced bond switching.

Why is the photoinduced-reorientation-based holographic most efficient at $\Lambda=10$ μm (Fig. 2)? This can be due to the collective character of the photoinduced bond reorientation process making it energetically profitable.[25] There may exist an optimal correlation domain size like in the collective photoinduced reorientation process of the chromophores in liquid-crystalline azobenzene side-chain polyesters.[53]

The dip in $\eta_{1\max}$ versus Λ dependence at $\Lambda\approx1$ μm (Fig. 2) can be explained by the Λ dependence of the photostimulated RSC. They counteract the reorientation processes and by assuming that they are most efficient around $\Lambda=1$ μm we can explain existence of the dip. Previously we have measured[18] that RSC initiated by PSC are the most efficient at $\Lambda=0.5$ μm. When $\Delta<0.5$ μm the proximity effect caused the decrease of the RSC. However, RSC caused by the photoinduced viscosity decrease during the 632.8 nm recording is a different less efficient process and can have the efficiency maximum shifted toward the longer period side because of the greater influence of the proximity.

Although the proposed explanation enables one to understand many features of the 632.8 nm holographic recording in a-As_2S_3 films it is still far from being fully clear. Not only the $\eta_{1\max}$ versus Λ dependence but also the origin and the time dependence of the grating shift in the course of exposure remains to be solved.

V. CONCLUSIONS

The subband-gap light holographic recording in a-As_2S_2 films at room temperature is experimentally studied. It is found that the properties of this recording considerably differ from those of usual holographic recording in amorphous chalcogenide films based on PSC.

The subband-gap holographic grating recording in a-As_2S_3 films performed by the 632.8 nm HeNe-laser light exhibits the following characteristic features: photoinduced refractive index increase, weak photobleaching, the absence of photoinduced thickness changes, a recording beam polarization dependence, oscillatory dependencies of the first order and the zeroth order diffraction efficiencies as functions of time, holographic grating shifts during the exposure, a peculiar two-maxima spatial frequency response, a lifetime of about two days, and the absence of the coherent hologram self-enhancement effect.[47] The first order diffraction efficiency up to 4.1% is achieved.

The mechanisms which are or can be used for holographic recording in amorphous chalcogenide films are analyzed. They include photostructural changes, photostimulated relaxational structural changes, photoinduced recharging of localized states in the bandgap and the photoinduced anisotropy. It is shown that only the photostimulated relaxational structure changes and the photoinduced anisotropy can give a significant contribution to the 632.8 nm recording in a-As_2S_3 films.

A mechanism is proposed to explain the subband-gap light holographic recording based on the photoinduced reorientation and generation of chalcogen related D^- and D^+ centers counteracted by the photostimulated relaxational structure changes.

Similar subband-gap light holographic recording processes can take place in other amorphous chalcogenide films. Their efficiency can probably be increased by heating.

ACKNOWLEDGMENTS

One of us (A.O.) is grateful to Professor T. Jääskeläinen for the possibility to perform these studies at the University of Joensuu. We would like to thank Dr. J. Teteris for consultations and providing the samples. These studies were supported by the Center of International Mobility (CIMO), Finland.

*FAX: +358 13 251 3212/3290. Electronic address: nordman@cc.joensuu.fi

[1] N. F. Mott and E. A. Davis, *Electronic Processes in Non-Crystalline Materials* (Clarendon, Oxford, 1979).
[2] K. Schwartz, *The Physics of Optical Recording* (Springer-Verlag, Berlin, 1993).
[3] G. Pfeiffer, M. A. Paesler, and S. C. Agarwal, J. Non-Cryst. Solids **130**, 111 (1991).
[4] V. N. Lyubin, in *Nonsilver Photographic Processes*, edited by A-L Kartuzhansky (Khimija, Leningrad, 1985), Chap. 8 (in Russian).
[5] *Amorphous Semiconductors*, edited by M. M. Brodskcy (Springer-Verlag, Berlin, 1979).
[6] B. Kumar and K. White, Thin Solid Films **135**, L13 (1986).
[7] M. Protasova and A. Ozols, Latvian J. Phys. Techn. Sci. **3**, 38 (1992).
[8] O. I. Shpotyuk, Phys. Status Solidi B **183**, 365 (1994).
[9] D. Turnbull, J. Non-Cryst. Solids **102**, 117 (1988).
[10] R. Ganesan, A. Srinivasan, K. N. Madhusoodanan, K. S. Sangunni, and E. S-R. Gopal, Phys. Status Solidi B **190**, K23 (1995).
[11] M. I. Klinger, Usp. Fiz. Nauk. **152**, 623 (1987).
[12] A. Z. Lowe, S. R. Elliot, and G. N. Greaves, Philos. Mag. B **54**, 483 (1986).
[13] K. J. Rao and R. Mohan, Solid State Commun. **39**, 1065 (1981).
[14] J. B. Raminez-Malo, E. Marquez, P. Villares, and R. Jimenez-Garay, Phys. Status Solidi A **133**, 499 (1992).
[15] J. Teteris, Phys. Status Solidi A **83**, K47 (1984).
[16] S. R Elliot, Nature **354**, 445 (1991).
[17] O. Salminen, N. Nordman, P. Riihola, and A. Ozols, Opt. Commun. **116**, 310 (1995).
[18] A. Ozols, O. Salminen, and M. Reinfelde, J. Appl. Phys. **75**, 3326 (1994).
[19] O. Salminen, A. Ozols, P. Riihola, and P. Mönkkönen, J. Appl. Phys. **78**, 718 (1995).
[20] A. Ozols, O. Salminen, P. Riihola, and P. Mönkkönen, J. Appl. Phys. **79**, 3397 (1996).
[21] A. Ozols, N. Nordman, and O. Nordman, Opt. Commun. (to be published).
[22] D. K. Tagantsev and S. V. Nemilov, Fiz. Khim. Stekla **15**, 397 (1989).
[23] H. Hisakuni and K. Tanaka, Science **270**, 974 (1995).
[24] S. Matsuoka, *Relaxation Phenomena in Polymers* (Hanser, Munich, 1992).
[25] D. Adler, in *Proceedings of the International Workshop on Amorphous Semiconductors*, Beijing, China, edited by M. Fritzshe, D.-X. Han, and C. C. Tsai (World Scientific, Singapore, 1987), pp. 3–14.
[26] F. Kosek, Z. Cimpl, J. Tulka, and J. Chlebny, J. Non-Cryst. Solids **90**, 401 (1987).
[27] J. Teteris and I. Manika, Latvian J. Phys. Techn. Sci. **2**, 3 (1995).
[28] S. A. Kolinko, V. M. Krishenik, O. V. Luksha, V. P. Ivanitsky, I. V. Prigara, and Yu. Yu. Firtsak, *Proceedings of the International Conference ''Non-Crystalline Semiconductors-89''*, Uzhgorad, USSR (Uzhgorod State University, Uzhgorod, 1989), Pt. I, pp. 240–242 (in Russian).
[29] R. A. Smith, *Semiconductors* (Cambridge University Press, Cambridge, England, 1978).
[30] E. Bustarret, J. Non-Cryst. Solids **114**, 13 (1989).
[31] Z. D. Jastrzebski, *The Nature and Properties of Engineering Materials* (Wiley, New York, 1987).
[32] M. Iijima and S. Kurita, J. Appl. Phys. **51**, 2103 (1980).
[33] F. Michelotti, E. Fazio, F. Senesi, M. Bertolotti, V. Chumash, and A. Andriesh, Opt. Commun. **101**, 74 (1993).
[34] A. V. Tyurin, A. Yu. Popov, V. E Mandel, and V. M. Belous, Solid State Phys. **38**, 379 (1996).
[35] L. E. Stis, Ukr. Fiz. Zh. **34**, 1688 (1989).
[36] H. Hisakuni and K. Tanaka, Appl. Phys. Lett. **65**, 2925 (1994).
[37] K. Tanaka, N. Toyosawa, and H. Hisakuni, Opt. Lett. **20**, 1976 (1995).
[38] V. G. Zhdanov and V. K. Malinovsky, Pis'ma Zh. Tehn. Fiz. **3**, 943 (1977) (in Russian).
[39] V. M. Lyubin and V. K. Tikhomirov, JETP Lett. **51**, 587 (1991).
[40] V. K. Tikhomirov, Phys. Tech. Semicond. **26**, 1415 (1992) (in Russian).
[41] V. M. Lyubini and V. K. Tikhomirov, J. Non-Cryst. Solids **171**, 87 (1994).
[42] V. Luibin and M. Klebanov, Phys. Rev. B **53**, R11 924 (1996).
[43] V. K. Tikhomirov and S. R. Elliot, Phys. Rev. B **51**, 5538 (1995).
[44] H. J. Eichler, P. Gunter, and D. W. Poahl, *Laser Induced Dynamic Gratings* (Springer-Verlag, Berlin, 1986), Chap. 4.
[45] A. Ozols, P. A. Augustov, and K. K. Shvarts, Opt. Spectrosc. (USSR) **44**, 683 (1978).
[46] H. Kogelnik, Bell Syst. Techn. J. **48**, 2909 (1969).
[47] A. Ozols, K. K. Shvarts, and M. J. Reinfelde, Proc. SPIE **1183**, 159 (1990).
[48] A. Ozols, Opt. Spectrosc. (USSR) **42**, 93 (1977).
[49] T. Suhara, H. Nishihara, and J. Koyama, Electron. Commun. Jpn. **59-C**, 116 (1976).
[50] W. Turalski, A. Miniewicz, and S. Bartkiewicz, Adv. Mat. Opt. Electron **6**, 15 (1996).
[51] V. M. Belous, V. E. Mandel, A. Yu. Popov, and A. V. Tyurin, Opt. Spectrosk. **76**, 105 (1974) (in Russian).
[52] J. Teteris and M. Reinfelde (unpublished).
[53] N. C. R. Holme, P. S. Ramanujam, and S. Hvilsted, Appl. Opt. **35**, 4622 (1996).